RSC Advances

ROYAL SOCIETY OF CHEMISTRY

www.rsc.org/advances

RSC Advances

RSCPublishing

ARTICLE

Controlled synthesis of highly stable zeolitic imidazolate framework-67 dodecahedra and their use towards the templated formation of hollow Co_3O_4 catalyst for CO oxidation

Cite this: DOI: 10.1039/x0xx00000x

Received 00th January 2012,
Accepted 00th January 2012

DOI: 10.1039/x0xx00000x

www.rsc.org/

Hongyu Wu,[a] Xukun Qian,[a,b,*] Haiping Zhu,[c] Songhua Ma,[a] Guangshan Zhu,[d] and Yi Long [b,*]

In this work, dodecahedral microcrystals of zeolitic imidazolate framework-67 (ZIF-67) with good uniformity and exceptional stability have been synthesized by simply controlling the mole ratio of reactants at room temperature. Field-emission scanning electron microscopy (FESEM) and transmission electron microscopy (TEM) characterizations indicate that the as-synthesized ZIF-67 microcrystals are highly uniform and have perfect rhombic dodecahedral morphology with 12 exposed {110} faces. The X-ray diffraction (XRD) and thermogravimetry analysis (TGA) investigations demonstrate that they display high thermal stability up to ~350 °C in air and ~425 °C in vacuum, as well as remarkable chemical resistance to boiling organic solvents and room-temperature water. Through two-step oxidative thermolysis process, these ZIF-67 dodecahedra can be further converted into hollow Co_3O_4 architectures consisting of nanosized building blocks. Owing to their large specific surface area and unique structure, the hollow Co_3O_4 catalyst obtained at the calcination temperature of 425 °C exhibits high catalytic activity and stability for gas-phase CO oxidation.

Introduction

As microporous crystals, zeolitic imidazolate frameworks (ZIFs)[1-5] are a new subclass of metal-organic frameworks (MOFs)[6-8] in which divalent metal cations are bonded with imidazolate anions into tetrahedral frameworks. ZIFs have attracted extensive attentions over the past few years owing to their large surface area, exceptional chemical and thermal stability.[1, 9] The outstanding properties enable them potential applications in various technological fields including gas sorption and separation,[10] molecular sieving,[11] chemical sensing,[12-13] drug delivery,[14] and heterogeneous catalysis.[15-17] Recently, MOFs/ZIFs have been proved to be ideal sacrificial templates to fabricate hollow metal oxides such as CuO,[7] Fe_2O_3[18-19] and Co_3O_4[20-21] mainly via thermolysis process under controlled atmosphere. The intrinsic porosity and long-range ordering within MOFs can offer a fast and convenient access for small molecules and ions diffusion during the transformation process. When evaluated as anode materials for lithium-ion batteries, these derived hollow metal oxides exhibit excellent electrochemical performance.[7,18-21]

In the past few years, many efforts have been carried out to control the size[22] and shape[23-24] of MOFs crystals since theses parameters can significantly influence their properties such as gas sorption[25] and indeed are critical for biological applications[26]. ZIF-8 ($Zn(mim)_2$, mim = 2-methylimidazolate) and ZIF-67 ($Co(mim)_2$) are two most representative members of the large ZIFs family.[2] They share quite similar crystal structure with a zeolite sodalite topology, which indicates they have similar crystallization mechanism. Syntheses of ZIF-8 with controlled particle sizes [3, 9, 27] and shapes [28-29] have been achieved in aqueous, methanol or dimethylformamide (DMF) solutions at room temperature. The obtained ZIF-8 particles usually are uniform and monodispersed and have large surface area of 800–1671 $m^2 \cdot g^{-1}$. Nevertheless, to our knowledge, only a few efforts have been devoted to the development of uniformly well-defined ZIF-67 so far. ZIF-67 has been synthesized under hydro-/solvothermal reaction between a cobalt salt and Hmim in solvents such as DMF[2] or water[28,30-31]. Nano-sized ZIF-67 crystals (~228 nm) were synthesized in aqueous solutions at room temperature.[30] The formation of ZIF-67 was accelerated and completed within 10 min by adding triethylamine to deprotonate the 2-methylimidazole (Hmim) linker. Unfortunately, these work failed to deliver uniform ZIF-67 crystals under the investigated conditions. To further tune the

[a] School of Engineering and Design, Lishui University, Lishui 323000, PR China. *E-mail: qianxukun@126.com*

[b] School of Materials Science and Engineering, Nanyang Technological University, Singapore 639798, Singapore. *E-mail: LongYi@ntu.edu.sg*

[c] School of Ecology, Lishui University, Lishui 323000, PR China.

[d] State Key Laboratory of Inorganic Synthesis and Preparative Chemistry, College of Chemistry, Jilin University, Changchun 130012, China

Electronic Supplementary Information (ESI) available: [details of any supplementary information available should be included here]. See DOI: 10.1039/b000000x/

properties of ZIF-67 for specific applications as well as to make them available as novel building blocks for advanced nanodevices, it is necessary to develop synthetic routes for the production of homogeneous crystals. Furthermore, controlling the shape and size of ZIF-67 particles will facilitate the fundamental understanding of the crystallization mechanism.

Chemical stability of ZIFs against aqueous or organic solutions is an important criterion for practical applications. One of the main advantages of ZIFs materials is their remarkable thermal and chemical stability when compared with other MOFs, a fact that undoubtedly expands their industrial applications in large scale.[1] The high chemical stability of ZIF-8 has been primarily attributed to the strong bonding between Zn(II) and mim(I). Another possible reason is that the hydrophobic pore and surface structure repels water molecules, preventing the attack of ZnN_4 units and dissolution of the framework.[1] In this regard, however, rather limited data have been reported on ZIF-67 in the scientific literatures up to now. This prompted us to make a systematic study on the stability of ZIF-67.

In this work, we report the facile synthesis of uniform and nonaggregated ZIF-67 dodecahedra. The thermal and chemical stability of the as-synthesized ZIF-67 microcrystals are also systematically examined using powder X-ray diffraction (XRD) and thermogravimetric analysis (TGA). By a two-step oxidative thermolysis of ZIF-67 templates, hollow Co_3O_4 catalysts with high specific surface area can be obtained, and they demonstrate remarkable catalytic activity for low-temperature CO oxidation.

Experimental

Materials

All chemicals purchased are of analytical grade and used without further purification.

Sample synthesis

To synthesize uniform and nonaggregated ZIF-67 crystals, $Co(NO_3)_2{\cdot}6H_2O$ and Hmim were separately dissolved in methanol. The concentrations of the $Co(NO_3)_2{\cdot}6H_2O$ and Hmim solutions were kept constant at 80 and 320 mM, respectively, while the molar ratio of Hmim/$Co(NO_3)_2{\cdot}6H_2O$ was varied from 4:1 to 32:1. The above two solutions were then mixed and stirred thoroughly for 30 s. Subsequently, the mixed solution was incubated without stirring at room temperature (RT) for 24 h. The supernatant was decanted away, and the purple precipitates were then collected by centrifugation followed by washing with methanol for three times. Finally they were vacuum-dried at 80 °C overnight.

Hollow Co_3O_4 dodecahedral catalysts consisting of nanoparticles were prepared via a two-step oxidative themolysis of ZIF-67 templates. First, the purple ZIF-67 powders were heated at a slow ramp of 5 °C·min^{-1} and then calcined in an inert atmosphere of flowing nitrogen for 30 min at 425, 500 and 575 °C, respectively. Subsequently, they were continuously calcined in an oxidative atmosphere of flowing air for another 30 min at the same temperature. Finally, the powders were cooled down naturally and the derived black products are correspondingly referred to as Co_3O_4-425, Co_3O_4-500 and Co_3O_4-575.

Characterization

TGA was performed on a NETZSCH STA449F3 thermoanalyzer. Samples were filled into aluminum crucibles and heated in vacuum/air with a ramp of 10 °C·min^{-1} from RT to 600 °C. Powder XRD data were collected on a Shimadzu XRD-6100 diffractometer with monochromatic Cu K_α radiation (λ = 1.540 Å). The scan speed was set to be 2°·min^{-1} in 2 theta.

The thermal stability of the as-synthesized ZIF-67 microcrystals in vacuum was monitored by *in-situ* Siemens D5005 high-temperature XRD diffractometer from RT to 450 °C. The diffractometer is equipped with monochromatic Cu K_α radiation (λ = 1.540 Å). The heating rate is 10 °C·min^{-1} and the scan speed 5°·min^{-1} in 2 theta.

The chemical stability of the as-synthesized ZIF-67 was studied by suspending the materials in boiling ethanol, toluene and boiling/RT water, respectively, for up to 7 days. After the treatment, the powders were centrifugated and vacuum-dried at 80 °C overnight before the XRD analysis was performed.

Nitrogen physisorption isotherms were measured on a Micromeritics ASAP 2020 volumetric instrument. Prior to the sorption measurements, ZIF-67 and templated hollow Co_3O_4 samples were degassed in vacuum at 100 °C for 12 h. Surface areas were estimated by applying the Brunauer-Emmett-Teller (BET) equation. The morphology and microstructure of the samples were characterized by a JEOL 7600F field-emission scanning electron microscopy (FESEM) at an acceleration voltage of 5 kV and a JEOL JEM-2100F high-resolution transmission electron microscopy (HRTEM) at an acceleration voltage of 200 kV.

The CO catalytic oxidation of templated hollow Co_3O_4 was evaluated in a fixed bed reactor at various temperatures without pre-treatment. 150 mg of the Co_3O_4 catalyst was sandwiched by two layers of quartz wool, and tested with the reaction gas, 1% CO balanced with air. The flow rate was fixed at 100 ml/min (GHSV= 110000 h^{-1}). The effluent gases in the outlet were analyzed online using an Shimadzu-14B gas chromatography equipped with TCD and FID detectors. The CO conversion was calculated from the measured CO concentration by the formula CO conversion = $[(CO_{in} - CO_{out})/CO_{in}] \times 100\%$, where CO_{in} and CO_{out} are the inlet and outlet CO concentration, respectively.

Results and discussion

The XRD patterns (Figure 1a) of the purple powders match well with the simulated and the published patterns,[28] indicating that all products are of phase-pure ZIF-67 materials. The narrow and strong peaks show that the as-synthesized ZIF-67 has high crystallinity. Interestingly, it is observed that the XRD pattern of ZIF-67 is nearly the same as that of ZIF-8[14], probably due to the rather similar crystal structure with a zeolite sodalite topology. The size and morphology of the as-synthesized ZIF-67 crystals were revealed by FESEM, as shown in Figure S1 a-d. Dodecahedral crystals formed when the mole ratio of Hmim/$Co(NO_3)_2{\cdot}6H_2O$ is 8:1 appear uniform and have a narrow size distribution (~ 1.5 μm). This suggests that ZIF-67 quickly nucleates in a very short time and grows at a slow rate in size without the occurrence of new (or secondary) nucleation. It is worth to note that Hmim is used in excess to the cobalt source in the present work. As previously reported, Hmim can act not only as a

linker unit in its deprotonated form but also as a stabilizing unit in its neutral form.[3] Excessive neutral Hmim in proper amount will probably be beneficial for synthesizing uniform ZIF-67 crystals. In comparison with previous synthesis of uniform and monodispersed MOFs crystals which involve complicated process,[32-35] our method can yield uniform ZIF-67 microcrystals by simply controlling the reactants' mole ratio without the addition of any auxiliary modulator such as capping agent, surfactants or polymers. The dry ZIF-67 powders are easily re-dispersed in methanol without any aggregations (Figure S1e). FESEM and TEM images (Figure 1b and c) reveal that the well-defined ZIF-67 crystals exhibit a rhombic dodecahedral shape with 12 exposed {110} faces, which is a special crystal form of the crystallographic point group $\bar{4}3m$. When viewed directly on a {110} face, the rhombic ZIF-67 dodecahedra appears with a hexagonal cross-section, the same as ZIF-8.[35] The N_2 adsorption measurement for the activated sample (Figure 1d) shows a reversible type I isotherm with an abrupt increase of the absorbed N_2 volume at relative low pressure (< 0.01), thereby suggesting a microporous nature. The microporous volume is 0.59 cm^3/g determined at P/P_0 = 0.10. Fitting the N_2 isotherms yields a BET surface area of 1587 m^2/g, a value much larger than that of ZIF-67 nanocrystals (316 m^2/g)[30] and comparable to that of ZIF-8 (1643 m^2/g)[14]. This provides proof of the highly accessible open pores within the crystal structure.

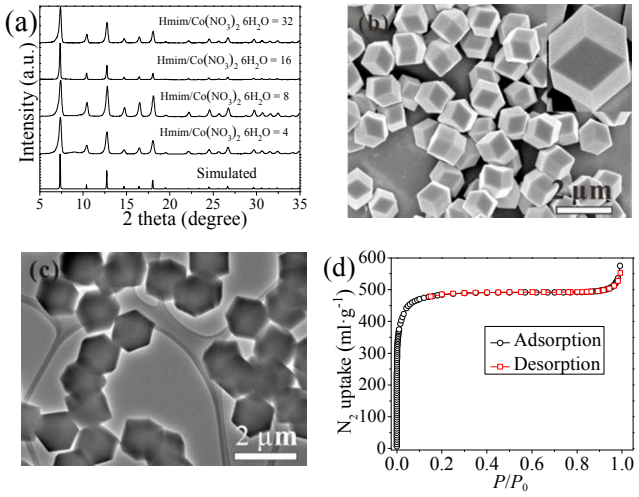

Figure 1 (a) XRD patterns of the as-synthesized ZIF-67 samples and the simulated one, (b) and (c) FESEM and TEM images of the dodecahedral ZIF-67 micorcrystals, (d) Nitrogen physisorption isotherms of the as-synthesized ZIF-67.

TGA curve (Figure 2a) of the as-synthesized material shows only ~3.1 wt % of guest molecules remained in the crystal pores. It is seen that ZIF-67 show different thermal stability in air and in vacuum. The ZIF-67 microcrystals are thermally stable up to ~350 °C and undergo fast decomposition at ~362 °C in air. However, they are thermally stable up to a higher temperature of ~425 °C in vacuum. The TGA results demonstrate that the as-synthesized ZIF-67 exhibits a higher thermal stability in vacuum than in air, indicating the framework structure is quite sensitive to oxygen at high temperature. Although the thermal stability of ZIF-67 in air is slightly lower than that of ZIF-8 (~500 °C),[12] it still surpasses many MOFs.[36] The thermal stability and decomposition in vacuum of ZIF-67 materials were further monitored by *in situ* high-temperature XRD, as shown in Figure 2b. Initially, the materials are able to maintain good crystalline up to 350 °C. A decrease in the peak intensity at 400 °C is observed, indicating the crystal decomposition occurred. As the temperature is increased to 425 °C, the diffraction peaks become much weaker. Finally, no diffraction peaks associated with ZIF-67 can be detected at 450 °C, clearly showing the completed decomposition of the material. These results are in accordance with the TGA analysis.

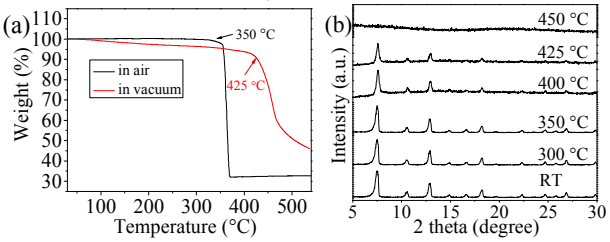

Figure 2 (a) TGA curve of the as-synthesized ZIF-67 samples, (b) *in situ* high-temperature XRD patterns of ZIF-67 microcrystals in vacuum.

Structural resistance to solvents is critical for the promising application of ZIFs. The chemical stability of dodecahedral ZIF-67 was examined by suspending powder samples in boiling ethanol, toluene and RT/boiling water, conditions that can represent operational parameters of typical chemical processes for industrial applications. The structure integrity of ZIF-67 after chemical treatment was monitored by XRD. As shown in Figure 3a, there is no significant change in the crystallinity level and peak positions for the tested crystals, nor is structural transformation observed after uninterrupted soaking. This proves that the as-synthesized ZIF-67 materials are stable in boiling ethanol for at least 7 days. In the case of boiling toluene, an obvious decrease in intensity of the (001) reflection (2θ = 7.335°) is observed. However, ZIF-67 still maintains its full crystallinity for 7 days. The highly chemical stability enables ZIF-67 as a potential catalyst or catalyst support for Knoevenagel reaction, where chemical reactions are normally performed in toluene.[37] Furthermore, ZIF-67 can also sustain its structure in RT water for 7 days (Figure S2). This good resistance to hydrolysis is comparable to that of ZIF-8 and UiO-66,[1, 38] and better than the well-known HKUST-1[39] and MOF-5[40-41]. To comprehensively investigate the chemical stability, ZIF-67 was further subjected to boiling water. An extra diffraction peak (2θ = 19.058) appears after soaking for 1 day and becomes stronger after prolonged soaking (Figure 3c). This suggests that ZIF-67 undergoes a gradual structural transformation and thus exhibits limited structure stability in boiling water. Finally, ZIF-67 crystals are completely transformed to other crystalline materials after 7 days because no peaks associated with them are detected. The wide angle XRD show the final product is composed of a mixture of Co_3O_4 and $Co(OH)_2$. Combined the FESEM examinations (Figure 3d) with EDS results (not shown here), it can be concluded that the spherical particle is Co_3O_4 whereas the plate-like crystal is $Co(OH)_2$. To the best of our knowledge, this is the first systematic study on the chemical stability of dodecahedral ZIF-67 crystals.

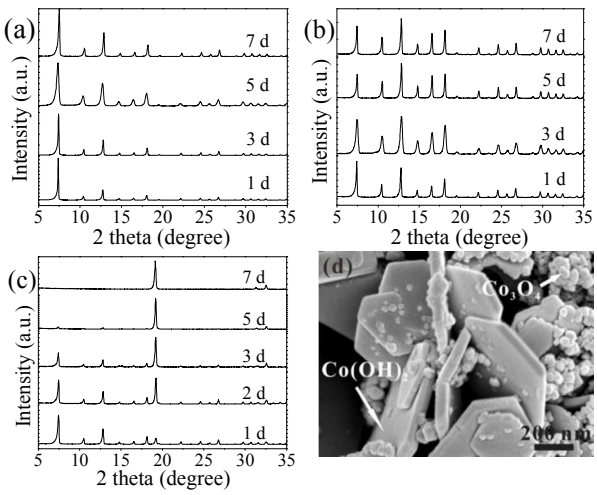

Figure 3 XRD patterns of the as-synthesized ZIF-67 samples soaking in different solutions: (a) boiling ethanol, (b) boiling toluene, (c) boiling water and (d) FESEM image of the samples after soaking in boiling water for 7 days.

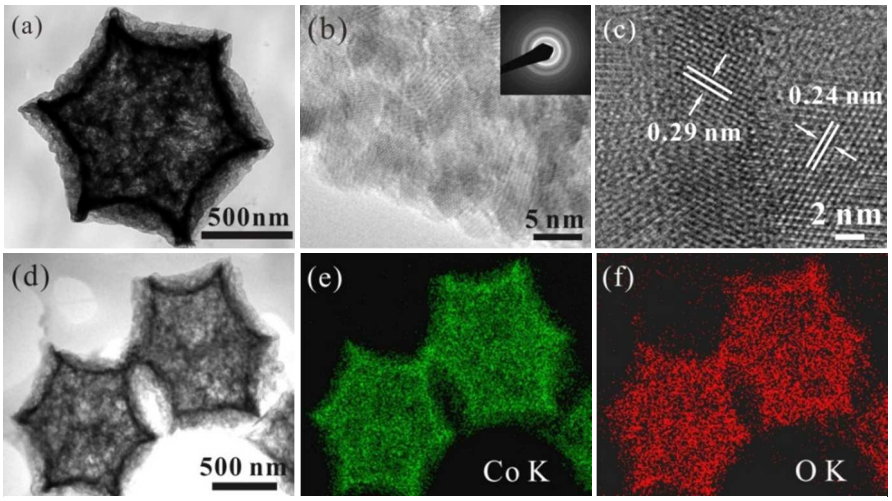

Figure 4 (a) low- and (b) high-magnified TEM images with inset showing SAED pattern of hollow Co_3O_4-425 dodecahedra, (c) HRTEM image of Co_3O_4 nanoparticles, (d) TEM image and (e, f) EDX-elemental mapping images of hollow Co_3O_4-425 dodecahedra.

Spinel cobalt oxide (Co_3O_4) has been extensively studied as heterogeneous catalysts,[42-43] anode materials in supercapacitors and lithium ion battery,[44-45] and gas sensing materials.[46] Highly symmetric hollow dodecahedra was obtained by a two-step oxidative thermolyis of dodecahedral ZIF-67 templates. In this transformation process, calcination conditions (e.g., temperature and atmosphere) can significantly affect the phase composition and microstructure of the finally derived products. The XRD results (Figure S4) show only Co_3O_4 exists in the final transformed products. There is no structure change in the temperature range of 425 to 575 °C. Therefore the catalysts are at least thermally stable up to 575 °C in air, which would be sufficient for catalytic conversion of CO. Typical morphologies of the hollow Co_3O_4 calcined at different temperatures are shown in Figure S5. After calcining the dodecahedral ZIF-67 microcrystals at the lower temperature of 425 °C (Figures 4a and S5a), the obtained Co_3O_4-425 products perfectly retain the geometries of the ZIF-67 templates. The highly symmetric dodecahedral structures of Co_3O_4-425 can be observed distinctly and the hollow interiors are clearly revealed by the sharp contrast between the centers and edges of dodecahedra (Figure 4a). The interior structure of the hollow Co_3O_4-425 dodecahedra is further studied by TEM and selected area electron diffraction (SAED). The magnified TEM image reveals that the hollow structure is composed of nanoparticles that are identified as polycrystalline Co_3O_4 by SAED pattern (Figure 4b). The HRTEM image (Figure 4c) taken near the dodecahedra edge displays distinct lattice fringes with d spacings of 0.29 and 0.23 nm, which are in good agreement with the (220) and (311) lattice planes of Co_3O_4, respectively. The elemental mapping results confirm the co-existence and homogenous distribution of Co and O elements within the dodecahedra (Figures 4d-f). As the temperature increases to 500 °C, the products can only remain a basic framework of dodecahedra (Figure S5b). Ultimately, the framework structure completely collapses at 575 °C (Figure S5c). Some Co_3O_4 grains agglomerate and coarsen with irregular shape.

To explore the porosity of the hollow Co_3O_4 dodecahedra, N_2 adsorption-desorption isotherms were recorded (Figure S6). As mentioned above, the as-synthesized ZIF-67 microcrystals show typical microporous structure with a high surface area (Figure 1d). After oxidative themolysis of ZIF-67 templates, a significant reduction of surface area from 1587 m^2/g down to 100 m^2/g is observed in comparison with the original ZIF-67. Nevertheless, hollow Co_3O_4-425 still exhibits a high surface area of 63.85 m^2/g. The Co_3O_4-425 and Co_3O_4-500 products display a typical type IV isotherm with distinct hysteresis loops, which is typical for cage-type pores and indicative of the presence of mesoporous structures. The adsorbed N_2 volumes of Co_3O_4-425 and Co_3O_4-500 gradually increase in the range of P/P_0 = 0.5-0.9, indicating the formation of pores with different sizes. Co_3O_4-575 has the smallest surface area of 12.65 m^2/g, which is due to the collapse of hollow structure and grain coarsening.

To investigate the advantages of the hollow Co_3O_4 dodecahedra, we herein studied their catalytic oxidation of CO. The catalytic activity for CO oxidation as a function of reaction temperature is shown in Figure 5. Apparently, the catalytic activity follows the order of Co_3O_4-425 > Co_3O_4-500 > Co_3O_4-575. It is concluded that the catalytic activity of the templated Co_3O_4 catalysts increases with decreasing calcination temperature. Both Co_3O_4-425 and Co_3O_4-500 exhibit significant catalytic activity at RT, while the Co_3O_4-575 catalyst shows negligible activity. It is noticed that CO conversion over three catalysts is increased with the temperature increasing. The temperatures for 50% CO conversion are approximately 309.8, 329.2 and 342.9 K, respectively, for Co_3O_4-425, Co_3O_4-500 and Co_3O_4-575. 100% CO conversion is achieved at 358 K and 368 K for Co_3O_4-425 and Co_3O_4-500 catalysts, respectively. In contrast, full CO conversion was obtained only at 378 K for Co_3O_4-575. Our

results demonstrate that the Co_3O_4-425 sample is highly reactive towards CO oxidation. The better catalytic properties of Co_3O_4-425 could be attributed to its hollow structure and larger surface area, which offers the largest contact area with CO. The catalytic performances of the present samples are better than that of Co_3O_4 nanoparticles[47], porous ZnO/Co_3O_4[48], and Cu/Cu_2O composites[49].

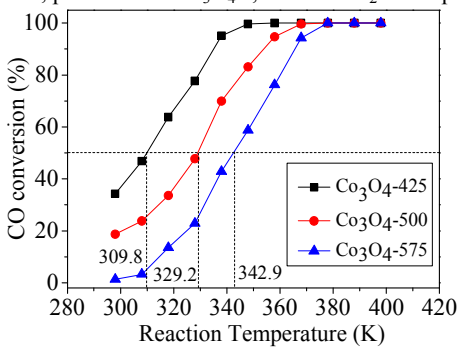

Figure 5 CO oxidation conversion as a function of reaction temperature.

As Co_3O_4 crystals may suffer from deactivation after long time reaction, the catalytic durability of the three catalysts was also evaluated (Figure 6). It is found that there is no significant loss of CO conversion after 20 h. The catalytic activity nearly remains unchanged. Therefore, the ZIF-67 templated Co_3O_4 catalysts exhibit good long-term stability. After the catalytic experiment, the recovered catalysts are subject to TGA test (Figure S7). It is seen there is no significant weight change during heating, which indicates the recovered catalyst is quite stable.

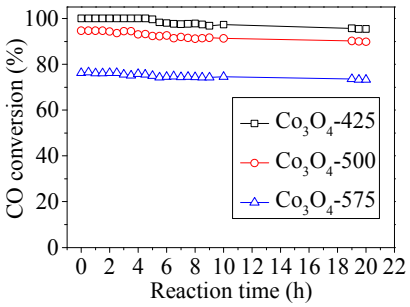

Figure 6 CO conversion of Co_3O_4 catalysts at 358 K with reaction time.

Conclusions

In summary, uniform dodecahedral ZIF-67 microcrystals were successfully synthesized by simply controlling the mole ratio of reactants at room temperature. Experimental results reveal that dodecahedral ZIF-67 is a robust porous material with excellent thermal and chemical stability. Taking advantage of the uniform and nonaggregated ZIF-67 microcrystals, hollow Co_3O_4 consisting of nanosized building blocks were successfully synthesized by heating ZIF-67 templates in controlled atmosphere. These hollow Co_3O_4 catalysts were examined to perform good catalytic activity and long-term stability for CO oxidation. This ZIF-templated synthetic strategy is believed feasible to fabricate other hollow metal oxides with well-defined structures, which will find more applications in catalysis, energy storage and conversion.

Acknowledgements

This research is financially supported by the project funded by the National Natural Science Foundation of China (11547028), the China Postdoctoral Science Foundation (2015M571865), the Preferred Fund of Postdoctoral Scientific Research Project of Zhejiang Province, the Opening Project of State Key Laboratory of Inorganic Synthesis and Preparative Chemistry (2015-13), the Opening Project of State Key Laboratory of Silicon Materials (SKL2015-05), the Campus for Research Excellence and Technological Enterprise (CREATE) programme, and Start-up Grant of the Nanyang Technological University (Grant No. SUG 10/10), Singapore.

Notes and references

1 X. Duan, H.Z. Wang, Y.J. Cui, Y. Yang, Z.Y. Wang, B.L. Chen and G.D. Qian, *RSC Adv.*, 2015, 5, 84446-84450.
2 C.S. Wu, Z.H. Xiong, C. Li and J.M. Zhang, *RSC Adv.*, 2015, 5, 82127-82137.
3 C.S. Lai, Y.F. Yeong, K.K. Lau and A.M. Shariff, *RSC Adv.*, 2015, 5, 79098-79106.
4 R.B. Wu, D.P. Wang, X.H. Rui, B. Liu, K. Zhou, A.W.K. Law, Q.Y. Yan and Z. Chen, *Adv. Mater.*, 2015, 27, 3038-3044.
5 R.B. Wu, D.P. Wang, V. Kumar, K. Zhou, P.S. Lee, A.W.K. Law, J. Lou and Z. Chen, *Chem. Commun.*, 2015, 51, 3109-3112.
6 R.B. Wu, D.P. Wang, J.Y. Han, H. Liu, K. Zhou, Y.Z. Huang, R. Xu, J. Wei, X.D. Chen and Z. Chen, *Nanoscale*, 2015, 7, 965-974.
7 R.B. Wu, X.K. Qian, F. Yu, H. Liu, K. Zhou, J. Wei and Y.Z. Huang, *J. Mater. Chem. A*, 2013, 1, 11126-11129.
8 X.K. Qian, B.L. Yadian, R.B. Wu, Y. Long, K. Zhou, B. Zhu and Y.Z. Huang, *Int. J. Hydrogen Energ.*, 2013, 38, 16710-16715.
9 Y.C. Pan, Y.Y. Liu, G.F. Zeng, L. Zhao and Z.P. Lai, *Chem. Commun.*, 2011, 47, 2071-2073.
10 Z.J. Zhang, S.K. Xian, H.X. Xi, H.H. Wang and Z. Li, *Chem. Eng. Sci.*, 2011, 66, 4878-4888.
11 C. Zhang, R.P. Lively, K. Zhang, J.R. Johnson, O. Karvan and W.J. Koros, *J. Phys. Chem. Lett.*, 2012, 3, 2130-2134.
12 S. Liu, Z.H. Xiang, Z. Hu, X.P. Zheng and D.P. Cao, *J. Mater. Chem.*, 2011, 21, 6649-6653.
13 Y. Hwang, H. Sohn, A. Phan, O.M. Yaghi and R.N. Candler, *Nano Lett.*, 2013, 13, 5271-5276.
14 G. Lu, S.Z. Li, Z. Guo, O.K. Farha, B.G. Hauser, X.Y. Qi, Y. Wang, X. Wang, S.Y. Han, X.G. Liu, J.S. DuChene, H. Zhang, Q.C. Zhang, X.D. Chen, J. Ma, S.C.J. Loo, W.D. Wei, Y.H. Yang, J.T. Hupp and F.W. Huo, *Nat. Chem.*, 2012, 4, 310-316.
15 C.M. Miralda, E.E. Macias, M.Q. Zhu, P. Ratnasamy and M.A. Carreon, *ACS Catal.*, 2012, 2, 180-183.
16 R.B. Wu, X.K. Qian, K. Zhou, H. Liu, B. Yadian, J. Wei, H.W. Zhu and Y.Z. Huang, *J. Mater. Chem. A*, 2013, 1, 14294-14299.

17 X.K. Qian, Z.Y. Zhong, B.L. Yadian, J.S. Wu, K. Zhou, J.S.K. Teo, L.W. Chen, Y. Long and Y.Z. Huang, *Int J Hydrogen Energ*, 2014, 39, 14496-14502.
18 X.D. Xu, R.G. Cao, S. Jeong and J. Cho, *Nano Lett*, 2012, 12, 4988-4991.
19 L. Zhang, H.B. Wu, S. Madhavi, H.H. Hng and X.W. Lou, *J Am Chem Soc*, 2012, 134, 17388-17391.
20 R.B. Wu, X.K. Qian, X.H. Rui, B.L. Yadian, K. Zhou, J. Wei, Q.Y. Yan, X.Q. Feng, Y. Long, L.Y. Wang and Y.Z. Huang, *Small*, 2014, 10, 1932-1938.
21 R.B. Wu, X.K. Qian, K. Zhou, J. Wei, J. Lou and P.M. Ajayan, *ACS Nano*, 2014, 8, 6297-6303.
22 L.G. Qiu, Z.Q. Li, Y. Wu, W. Wang, T. Xu and X. Jiang, *Chem. Commun.*, 2008, 3642-3644.
23 A. Schaate, P. Roy, A. Godt, J. Lippke, F. Waltz, M. Wiebcke and P. Behrens, *Chem. Eur. J.*, 2011, 17, 6643-6651.
24 Y.C. Pan, D. Heryadi, F. Zhou, L. Zhao, G. Lestari, H.B. Su and Z.P. Lai, *CrystEngComm*, 2011, 13, 6937-6940.
25 D. Tanaka, A. Henke, K. Albrecht, M. Moeller, K. Nakagawa, S. Kitagawa and J. Groll, *Nat. Chem.*, 2010, 2, 410-416.
26 W.J. Rieter, K.M.L. Taylor and W.B. Lin, *J. Am. Chem. Soc.*, 2007, 129, 9852-9853.
27 K. Kida, M. Okita, K. Fujita, S. Tanaka and Y. Miyake, *CrystEngComm*, 2013, 15, 1794-1801.
28 A.F. Gross, E. Sherman and J.J. Vajo, *Dalton Trans.*, 2012, 41, 5458-5460.
29 N. Yanai and S. Granick, *Angew. Chem. Int. Edit.*, 2012, 51, 5638-5641.
30 J.F. Qian, F.A. Sun and L.Z. Qin, *Mater. Lett.*, 2012, 82, 220-223.
31 Q. Shi, Z.F. Chen, Z.W. Song, J.P. Li and J.X. Dong, *Angew. Chem. Int. Edit.*, 2011, 50, 672-675.
32 G. Lu, C.L. Cui, W.N. Zhang, Y.Y. Liu and F.W. Huo, *Chem. Asian J.*, 2013, 8, 69-72.
33 M. Sindoro, A.Y. Jee and S. Granick, *Chem. Commun.*, 2013, 49, 9576-9578.
34 N. Yanai, M. Sindoro, J. Yan and S. Granick, *J. Am. Chem. Soc.*, 2013, 135, 34-37.
35 J. Cravillon, R. Nayuk, S. Springer, A. Feldhoff, K. Huber and M. Wiebcke, *Chem. Mater.*, 2011, 23, 2130-2141.
36 G. Ferey, *Chem. Soc. Rev.*, 2008, 37, 191-214.
37 U.P.N. Tran, K.K.A. Le and N.T.S. Phan, *ACS Catal.*, 2011, 1, 120-127.
38 J.H. Cavka, S. Jakobsen, U. Olsbye, N. Guillou, C. Lamberti, S. Bordiga and K.P. Lillerud, *J. Am. Chem. Soc.*, 2008, 130, 13850-13851.
39 P. Kusgens, M. Rose, I. Senkovska, H. Frode, A. Henschel, S. Siegle and S. Kaskel, *Microporous Mesoporous Mater.*, 2009, 120, 325-330.
40 J.A. Greathouse and M.D. Allendorf, *J. Am. Chem. Soc.*, 2006, 128, 10678-10679.
41 J. Yang, A. Grzech, F.M. Mulder and T.J. Dingemans, *Chem. Commun.*, 2011, 47, 5244-5246.
42 L. Hu, K. Sun, Q. Peng, B. Xu and Y. Li, *Nano Res.*, 2010, 3, 363-368.
43 V. Panwar, A. Al-Nafiey, A. Addad, B. Sieber, P. Roussel, R. Boukherroub and S.L. Jain, *RSC Adv.*, 2015, 5, 88567-88573.
44 L. Liu, D. Fang, M. Jiang, J.P. Chen, T. Wang, Q. Wang, L.J. Dong and C.X. Xiong, *RSC Adv.*, 2015, 5, 73677-73683.
45 J.B. Zhu, L.F. Bai, Y.F. Sun, X.D. Zhang, Q.Y. Li, B.X. Cao, W.S. Yan and Y. Xie, *Nanoscale*, 2013, 5, 5241-5246.
46 Y.Y. Lu, W.W. Zhan, Y. He, Y.T. Wang, X.J. Kong, Q. Kuang, Z.X. Xie and L.S. Zheng, *ACS Appl. Mater. Interfaces*, 2014, 6, 4186-4195.
47 W.X. Wang, Y.W. Li, R.J. Zhang, D.H. He, H.L. Liu and S.J. Liao, *Catal. Commun.*, 2011, 12, 875-879.
48 L. Hu, P. Zhang, Y.K. Sun, S.X. Bao and Q.W. Chen, *ChemPhysChem*, 2013, 14, 3953-3959.
49 S.Y. Zhang, H. Liu, C.C. Sun, P.F. Liu, L.C. Li, Z.H. Yang, X. Feng, F.W. Huo and X.H. Lu, *J. Mater. Chem*. A, 2015,3, 5294-5298.

Graphical Abstract

Controlled synthesis of highly stable zeolitic imidazolate framework-67 dodecahedra and their use towards the templated formation of hollow Co_3O_4 catalyst for CO oxidation

Uniform ZIF-67 dodecahedra with high thermal and chemical stability were successfully synthesized by simply controlling the reactants' mole ratio. Dodecahedral Co_3O_4 hollow architectures can be prepared from ZIF-67 templates via thermolysis, and they show excellent catalytic performance for CO oxidation.